Scattering Enabled Retrieval of Green's Functions from Remotely Incident Wave Packets using Cross Correlations☆

Maarten V. de Hoop[a], Josselin Garnier[b], Sean F. Holman[a], and Knut Sølna[c]

[a]*Center for Computational and Applied Mathematics, Purdue University, 150 N. University Street, West Lafayette IN 47907, USA*
[b]*Laboratoire de Probabilités et Modèles Aléatoires & Laboratoire Jacques-Louis Lions, Université Paris 7, 2 Place Jussieu, 75251 Paris Cedex 05, France*
[c]*Department of Mathematics, University of California at Irvine, Irvine, CA 92697-3875, USA*

Abstract

We analyze the notion of "field-field" cross correlations associated with scattered coda waves or clutter, observed at pairwise distinct receivers, to obtain an "empirical" Green's function (EGF) with an emphasis on high-frequency body waves. The scattered waves are generated in a slab with random medium fluctuations by an incident wave packet below. Following the dyadic parabolic scaling of wave packets, and scaling the random fluctuations appropriately, we arrive at a description in terms of a system of Îto-Schrödinger diffusion models. Studying the Wigner distributions of the fields generated by these models, leads to a "blurring" transformation providing a complete characterization of the mentioned cross correlations.

1. Introduction

We analyze the notion of "field-field" cross correlations associated with scattered coda waves, observed at pairwise distinct receivers, to obtain an "empirical" Green's function (EGF) with an emphasis on high-frequency body wave reflections.

As a model configuration, we consider a slab in which random medium fluctuations occur. The bottom of the slab is bounded by a deterministic discontinuity (a smooth reflector). We consider waves incident from above the slab, and place our receivers within the slab to study the corresponding cross correlations. Otherwise, in the entire configuration the medium has a deterministic, smoothly varying component; to simplify the presentation, here, we assume this component to be constant and the slab to be flat.

The incident wave is decomposed into wave packets. Each wave packet contains a particular scale. The decomposition is used to select a scale in relation to the fluctuations component of the medium in the slab. Through localization in phase space, the propagation and scattering of an incident wave packet can be described by a coupled system of paraxial wave equations written in curvilinear coordinates (with an associated Riemannian metric) which are defined by the rays, initiated by points in the support of the wave packet, in the deterministic component of the medium. Thus, in principle, each incident wave packet generates its own system of paraxial wave equations. The accuracy of this description can be proven to improve with increasingly finer scales, which is the regime considered here. Indeed, we view the EGF in the context of parametrix constructions. The paraxial form of the system allows for the use of Îto's stochastic calculus (for Hilbert-space valued processes) to analyze the scattering due to the random fluctuations; indeed, it enables the closure of the hierarchy of moment equations.

The solution procedure of each coupled system of paraxial wave equations is based on an invariant embedding type approach, generating a transmission and a reflection operator capturing the scattering due to the random fluctuations in the medium. Thus we arrive at a coupled system of Riccati equations for the mentioned operator kernels. In the limit of fine scales (high "frequency") in the sense of distributions, we then obtain a decoupled system of *linear* Îto-Schrödinger equations for formally limiting transmission and reflection operator kernels, with a real-valued Brownian field; to be precise, only the moments of these kernels converge in the mentioned limit.

☆This research was supported by NSF ARRA grant DMS *****

The solutions to the Îto-Schrödinger equations define the transmitted and backscattered fields, at least their statistics. The transmitted field is partly coherent and partly incoherent; the backscattered field is weak and fully incoherent in the absence of a smooth (deterministic) reflector, while it is partly coherent and partly incoherent in the presence of such a reflector. We analyze the Wigner distributions of these fields. We obtain a description of cross correlations in terms of transformations of Green's functions evaluated in the deterministic component of the medium yielding the EGF; this EGF should be viewed as a parametrix, while the transformations represent diffusion or blurring. Locally transverse medium diversity aids in sharpening these transformations, while the wave packets accommodate uncertainty in phase space.

The idea of using ambient noise for the retrieval of a body-wave reflection response, in a planarly layered medium, dates back to Claerbout [3]. He also conjectured that, in general media, cross correlating ambient noise traces from two locations recaptures the wavefield at one of the locations, excited by a point source at the other location. An early example of a field application was reported by Scherbaum [12], who analyzed auto-correlations of recordings of low-magnitude earthquakes and generated so-called pseudo-reflection seismograms. In the past decade, the understanding of how cross-correlating diffuse fields recaptures the Green's function, has been an important topic of research [16, 14]. Cross correlating (diffuse) coda waves [2] and ambient seismic noise [13] resulted in the retrieval of surface waves observed at one station and excited at the other station; for a detailed study, see Yao *et al.* [17]. Furthermore, *turning* body waves have been observed in cross correlating ambient noise [11]; in an exploration seismology setting, *reflected* body waves have also been recovered by cross correlations [7]. The retrieval of direct and reflected body waves using teleseismic (S-wave) coda was discussed in Tonegawa *et al.* [15]. The exploitation of a scattering medium in capturing the Green's function by field-field cross correlations was studied by Derode *et al.* [6]. However, the mathematical analysis of field-field cross correlations in this setting from the point of view of stcohastic calculus has just begun. See [1] for a recent analysis in the case of a bounded region.

2. Scaling and assumptions

We consider acoustic waves propagating in $1 + d$ spatial dimensions. The governing equations are

$$\rho(z,\boldsymbol{x})\frac{\partial \boldsymbol{u}}{\partial t} + \nabla p = \boldsymbol{F}, \quad \frac{1}{K(z,\boldsymbol{x})}\frac{\partial p}{\partial t} + \nabla\cdot\boldsymbol{u} = 0, \tag{1}$$

where p is the pressure field, $\boldsymbol{u}$ is the velocity field, ρ is the density of mass, and K is the bulk modulus of the medium; $(z,\boldsymbol{x}) \in \mathbb{R}\times\mathbb{R}^d$ denote the space coordinates. The source is modeled by the forcing term $\boldsymbol{F}$. We consider a configuration in which a random slab occupies the region

$$\Omega_r = \{(z,\boldsymbol{x}),\ \boldsymbol{x}\in\mathbb{R}^d,\ -L \le z \le 0\},$$

and is sandwiched in between two homogeneous half spaces. The surface $z = 0$ is the top interface and the surface $-L < 0$ is the bottom or interior interface. The medium consists of a deterministic component and random fluctuations in the region Ω_r, which vary rapidly in space. To simplify the analysis, the deterministic component of the medium in Ω_r is assumed to be constant.

The medium is assumed to be matched at the top interface $z = 0$ (transparent boundary conditions). However, the interior interface can act as a smooth reflector and is part of the deterministic component of the medium. (This model naturally captures primary reflections if the random fluctuations were absent.) Indeed, we consider a mismatch at the bottom of the slab, $z = -L < 0$, which gives jump conditions at the interior interface. The deterministic component of the medium is thus given by

$$\frac{1}{K(z,\boldsymbol{x})} = \begin{cases} K_0^{-1} & \text{if } z \le -L,\\ K_1^{-1}\left(1+\nu(z,\boldsymbol{x})\right) & \text{if } z\in(-L,0),\\ K_1^{-1} & \text{if } z \ge 0,\end{cases} \qquad \rho(z,\boldsymbol{x}) = \begin{cases}\rho_0 & \text{if } z\le -L,\\ \rho_1 & \text{if } z\in(-L,0),\\ \rho_1 & \text{if } z\ge 0,\end{cases}$$

where the random field $\nu(z,\boldsymbol{x})$ models the medium fluctuations, with correlation length l_K. The deterministic wavespeed for $z > -L$ is $c_1 = \sqrt{K_1/\rho_1}$, and for $z < -L$ is $c_0 = \sqrt{K_0/\rho_0}$.

The source, $\boldsymbol{F}$, is located at $z = z_s \ge 0$; we assume, here, that $z_s = 0$ and write $\boldsymbol{F}(t,z,\boldsymbol{x}) = f_s(t,\boldsymbol{x})\delta(z - z_s)\boldsymbol{e}_z$, where $\boldsymbol{e}_z$ denotes the unit vector pointing in the z-direction, signifying a body force. We shall refer to waves propagating in the positive z direction as upgoing. The source generates downgoing waves which "propagate" through the random medium, are reflected by the interface at $z = -L$, and "propagate" up through the medium.

We use the Fourier transforms,

$$\chi(t, \boldsymbol{x}) = \frac{1}{(2\pi)^{d+1}} \iint \hat{\chi}(\bar{\omega}, \boldsymbol{\kappa})\, e^{-i(\bar{\omega}t + \boldsymbol{\kappa}\cdot\boldsymbol{x})}\, c_1 d\bar{\omega} d\boldsymbol{\kappa} = \frac{1}{2\pi} \int \check{\chi}(\bar{\omega}, \boldsymbol{x})\, e^{-i\bar{\omega}t}\, d\bar{\omega}.$$

Let $\hat{\chi}$ denote a window function supported in a box in the $(\bar{\omega}, \boldsymbol{\kappa})$ Fourier domain such that $\chi_\varepsilon(t, \boldsymbol{x}) = \chi(\varepsilon^{-4}t, \varepsilon^{-2}\boldsymbol{x})$ corresponds with a wave packet oriented in the z direction of scale k, $\varepsilon = 2^{-k/4}$, corresponding with a dyadic parabolic decomposition of phase space. (The support of $\hat{\chi}$ is a finite distance away from the $\bar{\omega} = 0$ axis.) We adjust the shape of wave packets by introducing the dimensionless parameter τ according to

$$\hat{\chi}_\tau(\bar{\omega}, \boldsymbol{\kappa}) = \hat{\chi}\left(\frac{\bar{\omega}}{\tau}, \boldsymbol{\kappa}\right);$$

τ controls both the central frequency and frequency bandwidth of χ_τ. Then $\chi_{\tau;\varepsilon}(t, \boldsymbol{x}) = \chi_\tau(\varepsilon^{-4}t, \varepsilon^{-2}\boldsymbol{x})$. The source is now assumed to be of the form

$$\boldsymbol{F}(t, z, \boldsymbol{x}) = \chi_{\tau;\varepsilon}(t, \boldsymbol{x})\, \delta(z) \boldsymbol{e}_z. \tag{2}$$

Thus the transverse width, R_0, of the source function is of order ε^2. This scaling is consistent with the paraxial regime, which will be discussed in the next section, in as much as that it generates the wave solution up to an error of order ε^2. We assume that

- the correlation length or radius of the fluctuations, l_K, is of the same order as R_0; this regime guarantees non-trivial interaction between the fluctuations of the medium and the waves;
- the propagation distance is of the order of L, which is of order 1; the ratio between the propagation distance and the correlation length of the fluctuations is of order ε^{-2}.

The wave packet has a central frequency of order 2^k. We will establish results which converge as $k \to \infty$, signifying the high-frequency regime.

Henceforth we shall assume non-dimensionalized units chosen such that the deterministic bulk modulus K_1 and density ρ_1 in the region Ω_r are one and, hence, the deterministic wavespeed $c_1 = \sqrt{K_1/\rho_1}$ and impedance $Z_1 = \sqrt{K_1\rho_1}$ are equal to one. We assume that $Z_0 = \sqrt{K_0\rho_0} \neq 1$. The medium fluctuations attain the scaled form

$$\frac{1}{K(z, \boldsymbol{x})} = \begin{cases} K_0^{-1} & \text{if } z \leq -L, \\ 1 + \varepsilon^3 \nu(\frac{z}{\varepsilon^2}, \frac{\boldsymbol{x}}{\varepsilon^2}) & \text{if } z \in (-L, 0), \\ 1 & \text{if } z \geq 0, \end{cases} \qquad \rho(z, \boldsymbol{x}) = \begin{cases} \rho_0 & \text{if } z \leq -L, \\ 1 & \text{if } z \in (-L, 0), \\ 1 & \text{if } z \geq 0, \end{cases}$$

where ν is a zero-mean, stationary random field with correlation length of order one and standard deviation of order one. We write

$$C(z, \boldsymbol{x}) = \mathbb{E}[\nu(z' + z, \boldsymbol{x}' + \boldsymbol{x})\nu(z', \boldsymbol{x}')], \tag{3}$$

$$C_0(\boldsymbol{x}) = \int_{-\infty}^{\infty} C(z, \boldsymbol{x})\, dz. \tag{4}$$

We assume that ν satisfies strong mixing conditions in z. The amplitude ε^3 of the fluctuations has been chosen so as to obtain an effective limit of order one when ε goes to zero. That is, if the magnitude of the fluctuations is smaller than ε^3, then the wave would propagate as if the medium were homogeneous, while if the order of magnitude is larger, then the wave would not penetrate the slab at all. The scaling that we consider here, controlled by the choice of wave packet, corresponds to the partly coherent regime.

3. Coupled system of paraxial equations, and transmisison and reflection operators

We eliminate the transverse components of the velocity field. Because both the medium and the source have transverse spatial variations at the scale ε^2, it is convenient to rescale the transverse coordinates accordingly, that is, $\varepsilon^2\boldsymbol{x} \to \boldsymbol{x}$. In the region Ω_r, we then introduce the directional decomposition in the deterministic medium component,

$$p(t,z,\varepsilon^2 \boldsymbol{x}) = \frac{1}{2\pi}\int \left(\check{a}^\varepsilon(\bar{\omega},z,\boldsymbol{x})e^{i\bar{\omega}\frac{z}{\varepsilon^4}} + \check{b}^\varepsilon(\bar{\omega},z,\boldsymbol{x})e^{-i\bar{\omega}\frac{z}{\varepsilon^4}}\right)e^{-i\bar{\omega}\frac{t}{\varepsilon^4}}\,d\bar{\omega}, \tag{5}$$

with complex amplitudes $\check{a}^\varepsilon$ and $\check{b}^\varepsilon$ representing, locally, up- and down-going wave constituents, respectively. We have used Cartesian coordinates, since the ray generated by initial conditions corresponding with the center of the wave packet is straight, along the z direction.

The wave-packet source enables the use of the paraxial approximation in the deterministic component of the medium with the above mentioned estimate, leading to the system for $z \in (-L, 0)$:

$$\frac{\partial \check{a}^\varepsilon}{\partial z} = \left[\frac{i\bar{\omega}}{2\varepsilon}\nu\left(\frac{z}{\varepsilon^2},\boldsymbol{x}\right) + \frac{i}{2\bar{\omega}}\Delta_{\boldsymbol{x}}\right]\check{a}^\varepsilon + e^{-2i\bar{\omega}\frac{z}{\varepsilon^4}}\left[\frac{i\bar{\omega}}{2\varepsilon}\nu\left(\frac{z}{\varepsilon^2},\boldsymbol{x}\right) + \frac{i}{2\bar{\omega}}\Delta_{\boldsymbol{x}}\right]\check{b}^\varepsilon, \tag{6}$$

$$\frac{\partial \check{b}^\varepsilon}{\partial z} = -e^{2i\bar{\omega}\frac{z}{\varepsilon^4}}\left[\frac{i\bar{\omega}}{2\varepsilon}\nu\left(\frac{z}{\varepsilon^2},\boldsymbol{x}\right) + \frac{i}{2\bar{\omega}}\Delta_{\boldsymbol{x}}\right]\check{a}^\varepsilon - \left[\frac{i\bar{\omega}}{2\varepsilon}\nu\left(\frac{z}{\varepsilon^2},\boldsymbol{x}\right) + \frac{i}{2\bar{\omega}}\Delta_{\boldsymbol{x}}\right]\check{b}^\varepsilon, \tag{7}$$

supplemented with the boundary conditions:

$$\check{b}^\varepsilon(\bar{\omega}, z = 0^-, \boldsymbol{x}) = -\frac{1}{2}\check{\chi}_\tau(\bar{\omega},\boldsymbol{x}), \tag{8}$$

$$\check{a}^\varepsilon(\bar{\omega}, z = (-L)^+, \boldsymbol{x}) = \mathcal{R}_0 e^{2i\bar{\omega}\frac{L}{\varepsilon^4}}\check{b}^\varepsilon(\bar{\omega}, z = (-L)^+, \boldsymbol{x}), \tag{9}$$

where $\mathcal{R}_0 = (Z_0 - 1)/(Z_0 + 1)$. We also have the jump condition across $z = -L$:

$$\check{b}^\varepsilon(\bar{\omega}, (-L)^-, \boldsymbol{x}) = \mathcal{T}_0 \check{b}^\varepsilon(\bar{\omega}, (-L)^+, \boldsymbol{x}),$$

where $\mathcal{T}_0 = 2Z_0^{1/2}/(1 + Z_0)$, and across $z = 0$:

$$\check{a}^\varepsilon(\bar{\omega}, 0^+, \boldsymbol{x}) = \check{a}^\varepsilon(\bar{\omega}, 0^-, \boldsymbol{x}).$$

In the deterministic case, with $\nu = 0$, it can be proven that this system decouples with solutions accurate up to order ε^2.

We invoke an invariant imbedding approach to obtain the representation valid for $-L < z < 0$:

$$\check{b}^\varepsilon(\bar{\omega}, (-L)^-, \boldsymbol{x}) = \mathcal{T}_0 \int \boldsymbol{\mathcal{T}}^\varepsilon(\bar{\omega}, -L, z, \boldsymbol{x}, \boldsymbol{x}')\check{b}^\varepsilon(\bar{\omega}, z, \boldsymbol{x}')\,d\boldsymbol{x}', \tag{10}$$

$$\check{a}^\varepsilon(\bar{\omega}, z, \boldsymbol{x}) = \mathcal{R}_0 e^{2i\bar{\omega}\frac{L}{\varepsilon^4}} \int \boldsymbol{\mathcal{R}}^\varepsilon(\bar{\omega}, -L, z, \boldsymbol{x}, \boldsymbol{x}')\check{b}^\varepsilon(\bar{\omega}, z, \boldsymbol{x}')\,d\boldsymbol{x}', \tag{11}$$

where the operators $\boldsymbol{\mathcal{T}}^\varepsilon$ and $\boldsymbol{\mathcal{R}}^\varepsilon$, defined through their kernels, satisfy a natural coupled system of operator Riccati equations which follow from the equations satisfied by the local amplitudes. In the scaling regime $\varepsilon \to 0$ we are able to deduce from this system a description in terms of effective white noise models for the transmission and reflection operators, at least on the level of moments. We describe this in the next section.

The formulation generalizes to curvilinear coordinates if the deterministic wave speed in the slab is no longer constant, and the rays are no longer straight, using techniques from microlocal analysis and harmonic analysis.

4. Îto-Schrödinger diffusion models for transmitted and backscattered fields

We center according to the travel time associated with the deterministic medium component (constant wave speed, here) and define the transmitted and reflected pressure fields by

$$p_{\mathrm{R}}^\varepsilon(s, \boldsymbol{x}) := p(2L + \varepsilon^4 s, 0^+, \varepsilon^2 \boldsymbol{x}), \tag{12}$$

$$p_{\mathrm{T}}^\varepsilon(s, \boldsymbol{x}) := p(L + \varepsilon^4 s, (-L)^-, \varepsilon^2 \boldsymbol{x}) \tag{13}$$

The field $p_{\rm T}^\varepsilon(s,\boldsymbol{x})$ is the field observed just below the bottom interface at $z=(-L)^-$; the field $p_{\rm R}^\varepsilon(s,\boldsymbol{x})$ is the field observed just above the top interface at $z=0^+$:

$$p_{\rm R}^\varepsilon(s,\boldsymbol{x}) = \frac{1}{2\pi}\int \check{a}^\varepsilon(\bar\omega,0^+,\boldsymbol{x})e^{-i\bar\omega s}\,d\bar\omega, \tag{14}$$

$$p_{\rm T}^\varepsilon(s,\boldsymbol{x}) = \frac{1}{2\pi}\int \check{b}^\varepsilon(\bar\omega,(-L)^-,\boldsymbol{x})e^{-i\bar\omega s}\,d\bar\omega \tag{15}$$

These fields are now characterized via effective scaling limit models for the transmission and reflection operators:

Proposition 4.1. *The processes $(p_{\rm T}^\varepsilon(s,\boldsymbol{x}))_{s\in\mathbb{R},\boldsymbol{x}\in\mathbb{R}^d}$, $(p_{\rm R}^\varepsilon(s,\boldsymbol{x}))_{s\in\mathbb{R},\boldsymbol{x}\in\mathbb{R}^d}$ converge in distribution as $\varepsilon\to 0$ in the space $C^0(\mathbb{R},L^2(\mathbb{R}^d,\mathbb{R}^2))\cap L^2(\mathbb{R},L^2(\mathbb{R}^d,\mathbb{R}^2))$ to the limit processes $(p_{\rm T}(s,\boldsymbol{x}))_{s\in\mathbb{R},\boldsymbol{x}\in\mathbb{R}^d}$, $(p_{\rm R}(s,\boldsymbol{x}))_{s\in\mathbb{R},\boldsymbol{x}\in\mathbb{R}^d}$ given by*

$$p_{\rm R}(s,\boldsymbol{x}) = -\frac{\mathcal{R}_0}{4\pi}\iint \check{\boldsymbol{\mathcal{R}}}(\bar\omega,-L,0,\boldsymbol{x},\boldsymbol{x}')\check{\chi}_\tau(\bar\omega,\boldsymbol{x}')\,d\boldsymbol{x}'e^{-i\bar\omega s}\,d\bar\omega, \tag{16}$$

$$p_{\rm T}(s,\boldsymbol{x}) = -\frac{\mathcal{T}_0}{4\pi}\iint \check{\boldsymbol{\mathcal{T}}}(\bar\omega,-L,0,\boldsymbol{x},\boldsymbol{x}')\check{\chi}_\tau(\bar\omega,\boldsymbol{x}')\,d\boldsymbol{x}'e^{-i\bar\omega s}\,d\bar\omega, \tag{17}$$

where $\mathcal{T}_0$ and $\mathcal{R}_0$, are the transmission, resp. reflection, coefficient of the interface at $z=-L$ and defined above. Furthermore, $L^2(\mathbb{R},L^2(\mathbb{R}^d,\mathbb{R}^2))=L^2(\mathbb{R}\times\mathbb{R}^d,\mathbb{R}^2)$. The operators $(\check{\boldsymbol{\mathcal{R}}}(\bar\omega,-L,z,\boldsymbol{x},\boldsymbol{x}'))_{z\in[-L,0]}$ and $(\check{\boldsymbol{\mathcal{T}}}(\bar\omega,-L,z,\boldsymbol{x},\boldsymbol{x}'))_{z\in[-L,0]}$ are the solutions of the following Itô-Schrödinger diffusion models:

$$\begin{aligned} d\check{\boldsymbol{\mathcal{R}}}(\bar\omega,-L,z,\boldsymbol{x},\boldsymbol{x}') &= \frac{i}{2\bar\omega}\left(\Delta_{\boldsymbol{x}}+\Delta_{\boldsymbol{x}'}\right)\check{\boldsymbol{\mathcal{R}}}(\bar\omega,-L,z,\boldsymbol{x},\boldsymbol{x}')\,dz \\ &\quad+\frac{i\bar\omega}{2}\check{\boldsymbol{\mathcal{R}}}(\bar\omega,-L,z,\boldsymbol{x},\boldsymbol{x}')\circ\left(dB(z,\boldsymbol{x})+dB(z,\boldsymbol{x}')\right), \end{aligned} \tag{18}$$

$$\begin{aligned} d\check{\boldsymbol{\mathcal{T}}}(\bar\omega,-L,z,\boldsymbol{x},\boldsymbol{x}') &= \frac{i}{2\bar\omega}\Delta_{\boldsymbol{x}'}\check{\boldsymbol{\mathcal{T}}}(\bar\omega,-L,z,\boldsymbol{x},\boldsymbol{x}')\,dz \\ &\quad+\frac{i\bar\omega}{2}\check{\boldsymbol{\mathcal{T}}}(k,-L,z,\boldsymbol{x},\boldsymbol{x}')\circ dB(z,\boldsymbol{x}'), \end{aligned} \tag{19}$$

with the initial conditions at $z=-L$:

$$\check{\boldsymbol{\mathcal{R}}}(\bar\omega,-L,z=-L,\boldsymbol{x},\boldsymbol{x}')=\delta(\boldsymbol{x}-\boldsymbol{x}'),\qquad \check{\boldsymbol{\mathcal{T}}}(\bar\omega,-L,z=-L,\boldsymbol{x},\boldsymbol{x}')=\delta(\boldsymbol{x}-\boldsymbol{x}').$$

The symbol $\circ$ stands for the Stratonovich stochastic integral, and $B(z,\boldsymbol{x})$ is a real-valued Brownian field with covariance

$$\mathbb{E}[B(z_1,\boldsymbol{x}_1)B(z_2,\boldsymbol{x}_2)]=\min\{z_1,z_2\}C_0(\boldsymbol{x}_1-\boldsymbol{x}_2). \tag{20}$$

Making use of the semigroup property of the effective operators we also find that the joint law for the direct arrival to the two points of observation located at $(-L_1,\varepsilon^2\boldsymbol{x}_1)$ and $(-L_2,\varepsilon^2\boldsymbol{x}_2)$, with $-L\le -L_2\le -L_1\le 0$, can be characterized by

$$p(-L_1+\varepsilon^4 s,-L_1,\varepsilon^2\boldsymbol{x}_1)\sim\frac{-1}{4\pi}\iint\check{\boldsymbol{\mathcal{T}}}(\bar\omega,-L_1,0,\boldsymbol{x}_1,\boldsymbol{x}')\check{\chi}_\tau(\bar\omega,\boldsymbol{x}')\,d\boldsymbol{x}'e^{-i\bar\omega s}d\bar\omega, \tag{21}$$

$$\begin{aligned} p(-L_2+\varepsilon^4 s,-L_1,\varepsilon^2\boldsymbol{x}_2)&\sim\frac{-1}{4\pi}\iint\check{\boldsymbol{\mathcal{T}}}(\bar\omega,-L_2,-L_1,\boldsymbol{x}_2,\boldsymbol{x}'')\check{\boldsymbol{\mathcal{T}}}(\bar\omega,-L_1,0,\boldsymbol{x}'',\boldsymbol{x}') \\ &\quad\times\check{\chi}_\tau(\bar\omega,\boldsymbol{x}')\,d\boldsymbol{x}'d\boldsymbol{x}''e^{-i\bar\omega s}d\bar\omega, \end{aligned} \tag{22}$$

We remark that we introduced reflection and transmission operators for the full slab segments $(-L,z)$, $z\in(-L,0)$. The effective transmission models for sub-slabs (z_1,z), $z_1\in(-L,0)$, $z\in(z_1,0)$ are defined in the same way:

$$\begin{aligned} d\check{\boldsymbol{\mathcal{T}}}(\bar\omega,-z_1,z,\boldsymbol{x},\boldsymbol{x}') &= \frac{i}{2\bar\omega}\Delta_{\boldsymbol{x}'}\check{\boldsymbol{\mathcal{T}}}(\bar\omega,-z_1,z,\boldsymbol{x},\boldsymbol{x}')\,dz \\ &\quad+\frac{i\bar\omega}{2}\check{\boldsymbol{\mathcal{T}}}(\bar\omega,-z_1,z,\boldsymbol{x},\boldsymbol{x}')\circ dB(z,\boldsymbol{x}'),\quad \check{\boldsymbol{\mathcal{T}}}(\bar\omega,-z_1,z=-z_1,\boldsymbol{x},\boldsymbol{x}')=\delta(\boldsymbol{x}-\boldsymbol{x}'), \end{aligned} \tag{23}$$

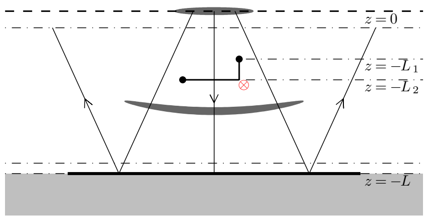

Figure 1: Configuration. The source is located at the surface $z = 0$. An interface is present at depth $-L$. We compute the correlation in between the two points at depth $-L_1$ and $-L_2$. The random fluctuations occur in the interval $z \in (-L, 0)$.

We note that, for $-L \le -L_2 \le -L_1 \le 0$, the operators $\check{\mathcal{T}}(\bar{\omega}, -L, -L_2, \boldsymbol{x}, \boldsymbol{x}')$ and $\check{\mathcal{R}}(\bar{\omega}, -L, -L_2, \boldsymbol{x}, \boldsymbol{x}')$ are statistically independent of $\check{\mathcal{T}}(\bar{\omega}, -L_2, -L_1, \boldsymbol{x}, \boldsymbol{x}')$ and $\check{\mathcal{R}}(\bar{\omega}, -L_2, -L_1, \boldsymbol{x}, \boldsymbol{x}')$, which we exploit in evaluating the cross-correlations. We remark here also that the transmission operator over the sub-slab $(-L_1, 0)$ appears in both expressions in (21-22) and it is this pairing that will lead to an expression for the cross correlations in terms of a statistically stable filter or transformation below. The general statistical properties of the operators $\check{\mathcal{R}}, \check{\mathcal{T}}$ were studied in [8].

5. Characterization of cross correlations and EGFs

Here, we characterize the "field-field" correlation function between the points $(-L_1, \varepsilon^2 \boldsymbol{x}_1)$ and $(-L_2, \varepsilon^2 \boldsymbol{x}_2)$. We assume here that $T \gg L$ and $0 < L_1 < L_2 < L$. The field-field correlation function is given by

$$\mathcal{V}_T^{\varepsilon}(\tau) = \int_0^T p(t, -L_1, \varepsilon^2 \boldsymbol{x}_1) p(t + \tau, -L_2, \varepsilon^2 \boldsymbol{x}_2)\, dt\,. \tag{24}$$

The configuration is illustrated in Figure 1, we compute the correlation in between the two points at depth $-L_1$ and $-L_2$. We will see that the wave field correlation function concentrates around specific time lags τ that correspond to travel times between the two observation points, and that the time extent of correlation function around these time lags is of order ε^4, i.e., of the same order as the source pulse width.

Under the scaling assumptions of Section 2 we find that the correlations in (24) has leading contributions at four particular times:

$$\mathcal{V}_T^{\varepsilon}(\,\pm (L_2 - L_1) + \varepsilon^4 s)/\varepsilon^4 \sim \mathcal{V}_{\rm t}^{\pm}(s)\,, \tag{25}$$
$$\mathcal{V}_T^{\varepsilon}(\,\pm (2L - L_1 - L_2) + \varepsilon^4 s)/\varepsilon^4 \sim \mathcal{V}_{\rm r}^{\pm}(s)\,. \tag{26}$$

Here, the amplitude scaling corresponds to a re-scaling of the source time traces so that they have order one energy, but plays no significant role as the problem is linear. We shall here focus on the contribution $\mathcal{V}_{\rm t}$ which corresponds to correlation of wave components directly transmitted in between the points of observation. The contribution at time lag equal to $+(L_2 - L_1)$ comes from the correlation between the waves that propagate from the surface to the depth $-L_1$ and then to the depth $-L_2$. The contribution at time lag equal to $-(L_2 - L_1)$ comes from the correlation between the waves that have been reflected by the interface at $z = -L$ and that propagate from this interface to the depth $-L_2$ and then to the depth $-L_1$. We stress here that these wave components have been strongly affected by the multiple scattering in the medium and understanding how this affects the relation of the components $\mathcal{V}$ and Green's functions is our main objective. The contribution $\mathcal{V}_{\rm r}$ corresponds to cross terms and it will be treated in detail elsewhere. We remark here that they give contributions for larger time lags than the first two contributions (since $2L - L_1 - L_2 > L_2 - L_1$) is larger than and could be used for estimation of the depth of the bottom interface.

The correlation component $\mathcal{V}_{\rm t}^{+}$ can be characterized in distribution in the scaling limit that we consider by the following expression using (21), (22) and the definition (24):

$$\mathcal{V}_{\rm t}^{+}(s) = \frac{1}{2\pi} \iint \Lambda_{\rm t}^{+}(\bar{\omega}, \boldsymbol{x}; \boldsymbol{x}_1) \check{\mathcal{T}}(\bar{\omega}, -L_2, -L_1, \boldsymbol{x}_2, \boldsymbol{x}_1 - \boldsymbol{x}) d\boldsymbol{x} e^{-iks} dk\,, \tag{27}$$

where $\check{\mathcal{T}}(\bar{\omega},-L,z,\boldsymbol{x},\boldsymbol{x}')$ is defined by (19). Remember that $\check{\mathcal{T}}(\bar{\omega},-L,z,\boldsymbol{x},\boldsymbol{x}')$ is the (rescaled) paraxial Green's function from the point $(z,\boldsymbol{x}')$ to the point $(-L,\boldsymbol{x})$. Therefore, (27) reads as a filtered version of the Green's function in between the two points of observation. This filter is

$$\Lambda_{\rm t}^{+}(\bar{\omega},\boldsymbol{x};\boldsymbol{x}_1)=\frac{1}{4}\iint\check{\mathcal{T}}(\bar{\omega},-L_1,0,\boldsymbol{x}_1-\boldsymbol{x},\boldsymbol{y}_2)\overline{\check{\mathcal{T}}(\bar{\omega},-L_1,0,\boldsymbol{x}_1,\boldsymbol{y}_1)}\check{\chi}_\tau(\bar{\omega},\boldsymbol{y}_2)\overline{\check{\chi}_\tau(\bar{\omega},\boldsymbol{y}_1)}d\boldsymbol{y}_1d\boldsymbol{y}_2. \tag{28}$$

In the regime we consider the filter $\Lambda_{\rm t}^{+}$ defining the relevant transformation is self-averaging [10] in the sense that

$$\begin{aligned}\Lambda_{\rm t}^{+}(\bar{\omega},\boldsymbol{x};\boldsymbol{x}_1) \quad = \quad & \frac{1}{4}\iint\mathbb{E}[\check{\mathcal{T}}(\bar{\omega},-L_1,0,\boldsymbol{x}_1-\boldsymbol{x},\boldsymbol{y}_2)\overline{\check{\mathcal{T}}(\bar{\omega},-L_1,0,\boldsymbol{x}_1,\boldsymbol{y}_1)}] \\ & \times\check{\chi}(\bar{\omega},\boldsymbol{y}_2)\overline{\check{\chi}(\bar{\omega},\boldsymbol{y}_1)}d\boldsymbol{y}_1d\boldsymbol{y}_2\,.\end{aligned}$$

In order to characterize the filter $\Lambda_{\rm t}^{+}$ we introduce the Wigner transform defined by

$$\begin{aligned}&W_{\bar{\omega}}^{T}(L_1,\boldsymbol{x},\boldsymbol{x}',\boldsymbol{\kappa},\boldsymbol{\kappa}')= \\ &\iint e^{-i(\boldsymbol{\kappa}\cdot\boldsymbol{y}+\boldsymbol{\kappa}'\cdot\boldsymbol{y}')}\mathbb{E}[\check{\mathcal{T}}\Big(\bar{\omega},-L_1,0,\boldsymbol{x}+\frac{\boldsymbol{y}}{2},\boldsymbol{x}'+\frac{\boldsymbol{y}'}{2}\Big)\overline{\check{\mathcal{T}}\Big(\bar{\omega},-L_1,0,\boldsymbol{x}-\frac{\boldsymbol{y}}{2},\boldsymbol{x}'-\frac{\boldsymbol{y}'}{2}\Big)}]d\boldsymbol{y}d\boldsymbol{y}'\,.\end{aligned}$$

The Wigner transforms can be shown to satisfy a set of transport equations that can be integrated [9] and we find the following integral representation for W^T:

$$W^{T}(z,\boldsymbol{x},\boldsymbol{x}',\boldsymbol{\kappa},\boldsymbol{\kappa}')=\frac{1}{(2\pi)^d}\iint e^{-i(\boldsymbol{\kappa}'+\boldsymbol{\kappa})\cdot\mathbf{a}-i(\boldsymbol{x}'-\boldsymbol{x}-\frac{\boldsymbol{\kappa}}{\bar{\omega}}L_1)\cdot\mathbf{b}}e^{\frac{\bar{\omega}^2}{4}\int_0^{L_1}C_0(\mathbf{a}+\frac{\mathbf{b}}{\bar{\omega}}z')-C_0(\mathbf{0})dz'}d\mathbf{a}d\mathbf{b}\,. \tag{29}$$

This gives then an integral expression for the filter. In order to get a explicit form for the filter and characterize the associated resolution scale, or filter support scale, we consider next a particular regime of relatively strong clutter.

The strongly cluttered regime

In the design of ν we introduce a relative stretch, l, of coordinates $(z,\boldsymbol{x})$ through it autocorrelation function. We write ν_l for the random field with autocorrelation function

$$C(z,\boldsymbol{x})=\sigma^2C\Big(\frac{z}{l},\frac{\boldsymbol{x}}{l}\Big),$$

where σ is the standard deviation of the fluctuations of the random medium. With this representation we have

$$C_0(\boldsymbol{x})=\sigma^2lC_0\Big(\frac{\boldsymbol{x}}{l}\Big).$$

We assume also that the autocorrelation function $C_0(\boldsymbol{x})$ is at least twice differentiable at $\boldsymbol{x}=\mathbf{0}$, which corresponds to a smooth random medium. Thus, we replace in the proposition ν by ν_l.

We introduce the parameter, depending on τ,

$$\beta_L(\tau)=L\frac{\sigma^2\tau^2l}{4}, \tag{30}$$

which characterizes the strength of the forward scattering. We shall then assume a subsequent scaling regime corresponding to relatively strong medium interaction, with $\beta_L(\tau)$ being large.

Second we introduce the resolution parameter:

$$\Sigma_{\bar{\omega}}^2(L_1)=\frac{l^2}{\beta_{L_1}(\bar{\omega})\mathcal{D}}=\frac{4}{\bar{\omega}^2DL_1}\,, \tag{31}$$

where we defined

$$D=\frac{\sigma^2\mathcal{D}}{l}=-\frac{1}{d}\triangle C_0(\mathbf{0})\,,\quad \mathcal{D}=-\frac{1}{d}\triangle C_0(\mathbf{0})\,.$$

Using [8] we find the following expression for the filter

$$\Lambda_{\rm t}^{+}(\bar{\omega}, \boldsymbol{x}; \boldsymbol{x}_1) = \frac{1}{4(24\pi D L_1^3)^{(d/2)}} \exp\Big(- \frac{|\boldsymbol{x}|^2}{2\Sigma_{\bar{\omega}}^2(L_1)} \Big) \int |\check{\chi}(\bar{\omega}, \boldsymbol{y}_1)|^2 d\boldsymbol{y}_1 \,. \tag{32}$$

Thus, we have a situation in which a sharp filter and Green's function estimation has been enabled by the medium correlations. We remark that the expression (32) is valid and is independent of $\boldsymbol{x}_1$ as long as the point $\boldsymbol{x}_1$ is in the forward cone of wave energy [8, 10], or of order $\mathcal{A}_{\rm eff}(L_1)$, for the effective aperture

$$\mathcal{A}_{\rm eff}(L_1) = \sqrt{D L_1^3} \,.$$

We have similarly

$$\mathcal{V}_{\rm t}^{-}(s) = \frac{1}{2\pi} \iint \Lambda_{\rm t}^{-}(\bar{\omega}, \boldsymbol{x}; \boldsymbol{x}_2) \check{\mathcal{T}}(\bar{\omega}, -L_1, -L_2, \boldsymbol{x}_1, \boldsymbol{x}_2 - \boldsymbol{x}) d\boldsymbol{x} e^{-i\bar{\omega}s} d\bar{\omega} \,,$$

with the filter

$$\Lambda_{\rm t}^{-}(\bar{\omega}, \boldsymbol{x}; \boldsymbol{x}_2) = \frac{1}{4} \iint \check{\mathcal{T}}(\bar{\omega}, -L_2, 0, \boldsymbol{z}_2, \boldsymbol{y}_2) \overline{\check{\mathcal{T}}(\bar{\omega}, -L_2, 0, \boldsymbol{z}_1, \boldsymbol{y}_1)}$$
$$\times \check{\mathcal{R}}(\bar{\omega}, -L, -L_2, \boldsymbol{x}_2, \boldsymbol{z}_2) \overline{\check{\mathcal{R}}(\bar{\omega}, -L, -L_2, \boldsymbol{x}_2 - \boldsymbol{x}, \boldsymbol{z}_1)} \check{\chi}(\bar{\omega}, \boldsymbol{y}_2) \overline{\check{\chi}(\bar{\omega}, \boldsymbol{y}_1)} d\boldsymbol{y}_1 d\boldsymbol{y}_2 \,.$$

Note that, by reciprocity, we have

$$\mathcal{V}_{\rm t}^{-}(s) = \frac{1}{2\pi} \iint \Lambda_{\rm t}^{-}(\bar{\omega}, \boldsymbol{x}; \boldsymbol{x}_2) \overline{\check{\mathcal{T}}(\bar{\omega}, -L_2, -L_1, \boldsymbol{x}_2 - \boldsymbol{x}, \boldsymbol{x}_1)} d\boldsymbol{y} e^{-i\bar{\omega}s} d\bar{\omega} \,, \tag{33}$$

which shows that we obtain a filtered version of the anti-causal Green's function in between the two points of observation.

We can also get a simple expression of the filter in the strongly cluttered regime. Self-averaging implies that

$$\Lambda_{\rm t}^{-}(\bar{\omega}, \boldsymbol{x}; \boldsymbol{x}_2) = \frac{\mathcal{R}_0^2}{4} \iint \mathbb{E}[\check{\mathcal{T}}(\bar{\omega}, -L_2, 0, \boldsymbol{z}_2, \boldsymbol{y}_2) \overline{\check{\mathcal{T}}(\bar{\omega}, -L_2, 0, \boldsymbol{z}_1, \boldsymbol{y}_1)}] \tag{34}$$
$$\times \mathbb{E}\Big[\check{\mathcal{R}}(\bar{\omega}, -L, -L_2, \boldsymbol{x}_2, \boldsymbol{z}_2) \overline{\check{\mathcal{R}}(\bar{\omega}, -L, -L_2, \boldsymbol{x}_2 - \boldsymbol{x}, \boldsymbol{z}_1)}\Big] \check{\chi}(\bar{\omega}, \boldsymbol{y}_2) \overline{\check{\chi}(\bar{\omega}, \boldsymbol{y}_1)} d\boldsymbol{y}_1 d\boldsymbol{y}_2$$

We will again in general have sharp clutter enabled resolution for the filter $\Lambda_{\rm t}^{-}$, analogously to the situation for the filter $\Lambda_{\rm t}^{+}$. However, the presence of the reflection operator in the expression for the filter (34) modifies the expression for the filter in a way that depends more critically on the particular scaling regime considered. In particular, one may have scaling situations in which there is a restoration of coherence for the reflected waves which affects the resolution, moreover, a diffusive or incoherent bottom interface condition will affect wave diversity and resolution, [9]. These phenomena will be treated in detail elsewhere.

6. Discussion

We presented an analysis for partly coherent and partly incoherent body waves generated by a (teleseismic) wave packet remotely incident on a slab (the crust) containing a medium consisting of a deterministic component and a random field, based on the dyadic parabolic decomposition of phase space coupled to the scaling of the random fluctuations. The deterministic component consists, here, of a planarly layered medium, but can be generalized to contain conormal singularities (discontinuities) combined with smooth wave speed variations. To obtain information about the deterministic medium component, one needs to consider "field-field" cross correlations. We showed that these cross correlations are characterized by a transformation (blurring filter) of the Green's function (parametrix) in the deterministic component of the medium, between the points at which the fields are taken, the transformation containing information about the statistics of the random fluctuations. If the points are taken purely transverse to the propagation direction of the wave packet in the deterministic component, the blurring significantly increases, which is consistent with the usual stationary phase arguments. In principle, incident packets also can be summed to form a point source, to represent local seismicity.

[1] C. Bardos, J. Garnier and G. Papanicoalou, *Identification of Green's function singularities by cross correlation of noisy signals*, preprint.

[2] M. Campillo and A. Paul, *Long-range correlations in the diffuse seismic coda*, Science, 299, 547-549, (2003).

[3] J. F. Claerbout, *Synthesis of a layered medium from its acoustic transmission response*, Geophysics, 33, 264-269, (1968).

[4] J. F. Claerbout, *Coarse grid calculations of waves in inhomogeneous media with application to delineation of complicated seismic structure*, Geophysics, 35, 407-418, (1970).

[5] A. Derode and M. Fink, *How to estimate the Green's function of a heterogeneous medium between two passive sensors? Application to acoustic waves*, Applied Physics Letters, V 83, 15, 3054-3056, (2003).

[6] A. Derode, E. Larose, M. Tanter, J. de Rosny, A. Tourin, M. Campillo and M. Fink, *Recovering the Green's function from field-field correlations in an open scattering medium*, J. Acoust. Soc. Am., 113, 2973-2976, (2003)

[7] D. Draganov, K. Wapenaar, W. Mulder, J. Singer and A. Verdel, *Retrieval of reflections from seismic background-noise measurements*, Geophys. Res. Lett., 34, L04305, doi:10.1029/2006GL028735, (2007).

[8] J. Garnier and K. Sølna, Coupled paraxial wave equations in random media in the white-noise regime, Ann. Appl. Probab. 19, 318-346 (2009).

[9] J. Garnier and K. Sølna, Scaling limits for wave pulse transmission and reflection operators, *Wave Motion*, 2, 122-143, 2009.

[10] M.V. de Hoop and K. Sølna, Estimating a Green's function from "field-field" correlations in a random medium, SIAM J. Appl. Math., 69, 909-932, 2009.

[11] P. Roux, K. G. Sabra, P. Gerstoft, W. A. Kuperman and M. Fehler, *P-waves from cross correlation of seismic noise*, Geophys. Res. Lett., 32, L19303, doi:10.1029/2005GL023803, (2005)

[12] F. Scherbaum, *Seismic imaging of the site response using micro-earthquake recordings. Part II: Application to the Swabian Jura, Sothwest Germany, seismic network*, Bull. Seismol. Soc. Am., 77, 1924-1944, (1987).

[13] N. M. Shapiro, M. Campillo, L. Stehly and M. Ritzwoller, High-Resolution Surface-Wave Tomography from Ambient Seismic Noise, Science, V 307, 11 March 2005.

[14] B. A. van Tiggelen, *Green function retrieval and time reversal in a disordered world*, Phys. Rev. Lett., 91 (243904), 1-4, (2003).

[15] T. Tonegawa, K. Nishida, T. Watanabe and K. Shiomi, *Seismic interferometry of teleseismic S-wave coda for retrieval of body waves: an application to the Philippine Sea slab underneath the Japanese Islands*, Geophys. J. Int., 178, 1574-1586, (2009).

[16] R. L. Weaver and O. I. Lobkis, *Ultrasonics without a source: Thermal fluctuation correlations at Mhz frequencies*, Phys. Rev. Lett. 93 (254301), 1-4, (2001).

[17] H. Yao, R. D. van der Hilst and M. V. de Hoop, *Surface-wave array tomography in SE Tibet from ambient seismic noise and two-station analysis – I. Phase velocity maps*, Geophys. J. Int., 166, 732-744, (2006).